S1. Data collection timeline

The observation period at Heron Island spanned early November to mid-December 2024. Instrument installation and testing took place from 2–5 November 2024, with all major instruments operational by 5 November. Continuous measurements were then conducted until 11 December 2024, when the campaign concluded. All data were recorded in UTC time (local time is UTC+10) to maintain consistent timestamps across instruments. Different instruments had slightly different operational periods and uptimes, which are noted in Table S1.

NAIS started logging on 2 Nov 2024 (12:00 UTC) but unfortunately suffered an electrical high-voltage breakdown on 16 Nov 2024, 03:30 UTC. After this failure, the NAIS could no longer collect valid size distribution data. However, it was kept powered on to avoid perturbing the inlet conditions. Thus, NAIS data are available only for the first two weeks of the campaign. VOCUS operated from 6 Nov 2024 (00:00 UTC) until 29 Nov 2024, 8:30 UTC. The NO_x analyzer ran from 2 Nov 2024 (16:50 UTC) through 4 Dec 2024 (23:00 UTC). Partway through the campaign (around 23 Nov), the NOx instrument began to overheat, necessitating periodic shutdowns to cool. From 23 Nov onward, data gaps appear whenever the instrument was off, and after 4 Dec the NOx analyzer remained off due to persistent overheating issues. Users of the NOx data should be cautious of these interruptions and the lack of data in the final week. Other instruments were run continuously from ~5 Nov 2024 (10:00 UTC) to 11 Dec 2024 (23:30 UTC). There were a few brief outages for maintenance, described below, but otherwise these datasets cover the full 5-week period.

Table S1. Overview of instruments deployed during the Heron Island 2024 campaign and their measuring periods.

Parameter	Instrument	Measurement time
Particle number size distribution	Scanning Electrical Mobility Spectrometer 10-1000 nm (SEMS, Brechtel, USA)	5th of November – 11th of December 2024
	Aerodynamic Particle Sizer 700-5000 nm (APS, TSI, USA)	5th of November – 11th of December 2024
	Neutral cluster and Air Ion Spectrometer (NAIS, Airel Ltd.)	2nd November – 16th of November 2024
Particle number concentration	Condensation Particle Counter (CPC, A20 Airmodus, Finland)	5th of November – 11th of December 2024
Cloud condensation nuclei concentration	Cloud Condensation Nuclei counter (CCN-100, Droplet Measurement Technologies, USA)	5th of November – 11th of December 2024
Chemical composition of non-refractory PM_1	Aerosol Mass Spectrometer (AMS, Aerodyne)	5th of November – 11th of December 2024
Chemical composition of volatile organic compounds	Vocus proton-transfer-reaction Time-of-Flight Mass Spectrometer (Vocus-PTR-ToF-MS, Aerodyne)	6th – 29th of November 2024
Black carbon concentration	Aethalometer (AE33, Aerosol Magee Scientific, Slovenia)	5th of November – 11th of December 2024
	Tricolour Absorption Photometer (TAP, Brechtel, USA)	5th of November – 11th of December 2024
CO_2 concentration	CO_2 analyser (840A, Li-COR)	5th of November – 11th of December 2024
NO_x concentration	NO_x analyser (9841A, Ecotech, Australia)	2nd of November – 4th of December 2024
O_3 concentration	O_3 analyser (9810B, Ecotech, Australia)	5th of November – 11th of December 2024
Meteorological parameters	Weather station (Gill MaxiMet GMX501, Gill Instruments Ltd., UK)	5th of November – 11th of December 2024
Inlet line parameters	RH and T sensor (HMP60, Vaisala)	5th of November – 11th of December 2024

S2. Corrections and calibration

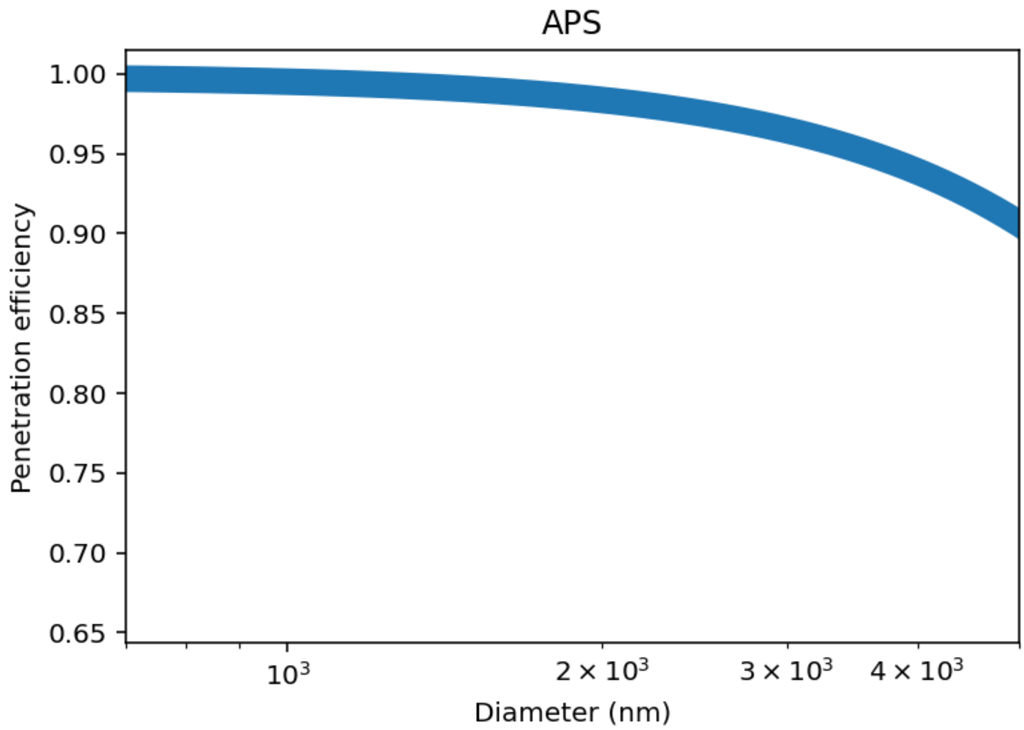

Figure S1: Particle penetration efficiency as a function of diameter for APS.

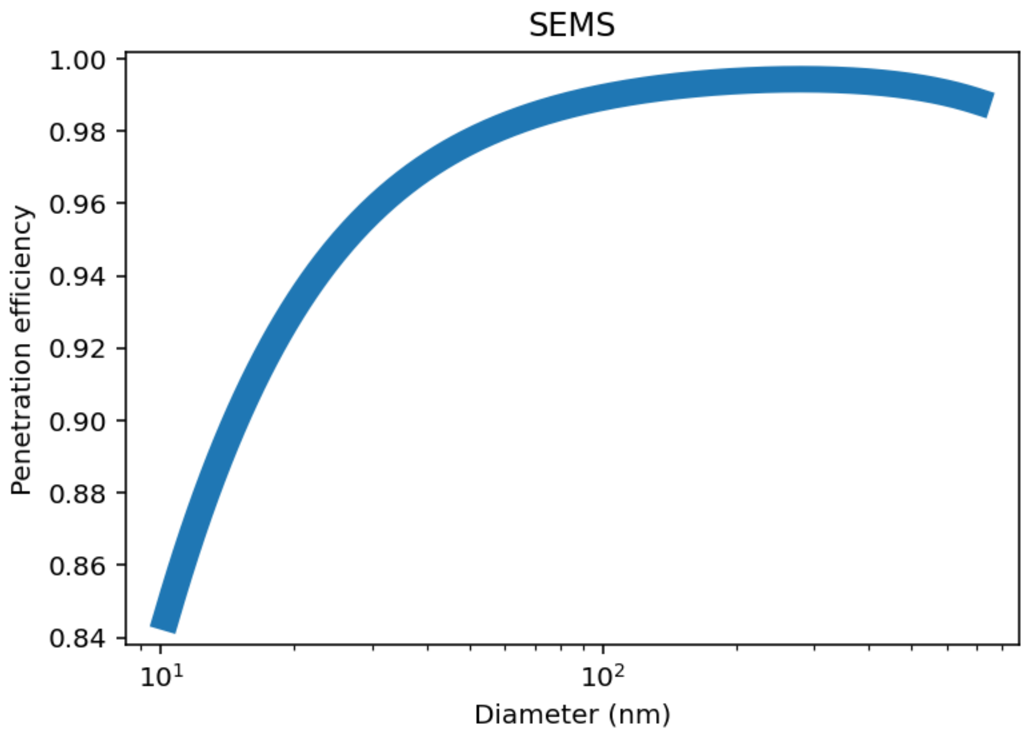

Figure S2: Particle penetration efficiency as a function of diameter for SEMS.

Table S2. List of compounds mixed into calibration gas mixture as well as their chemical formula, ion used for detection with Vocus-ToF-MS, and detection limit.

Compound	Formula	Detected ion	DL (ppb)	
			Before 18-11-2024	From 18-11-2024
Acetaldehyde	C2H4O	C2H5O+	0.440	
Acetonitrile	C2H3N	C2H4N+	1.400	
Acetone	C3H6O	C3H7O+	0.047	
Pentane	C5H12	C5H13+	0.010	
Isoprene	C5H9	C5H10+	0.018	
Dimethyl sulfide	C2H6S	C2H7S+	0.001	
Methyl Ethyl Ketone	C4H8O	C4H9O+	0.017	
Benzene	C6H6	C6H7+	0.014	
Cyclohexane	C6H12	C6H13+	7.400	3.000
Toluene	C7H8	C7H9+	0.050	
m, o - Xylene	C8H10	C8H11+	0.020	
a-Pinene	C10H16	C10H17+	0.010	
1,3,5-Trimethylbenzene	C9H12	C9H13+	0.010	

S3. Overview of measured and calculated variables

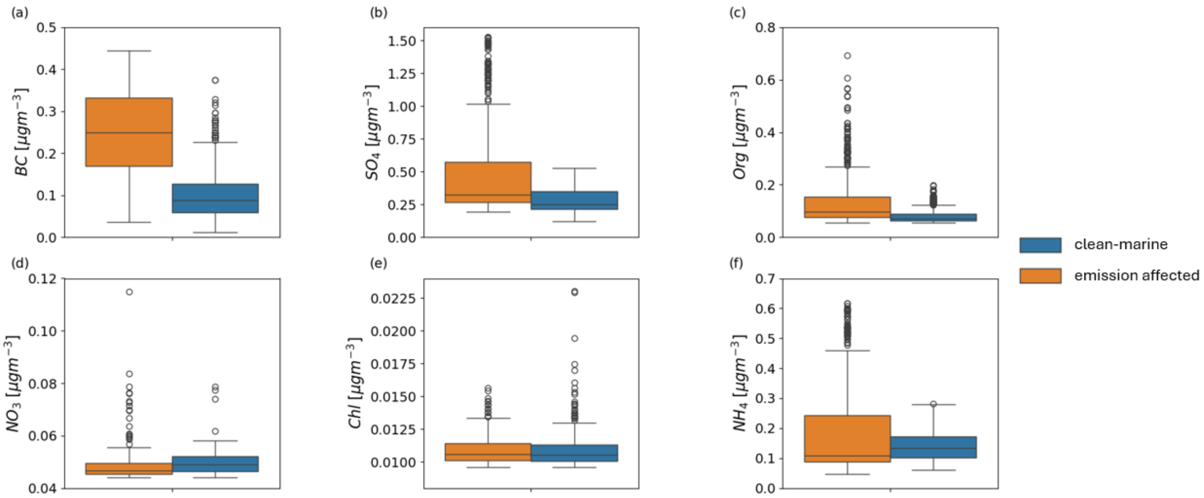

Figure S3: The chemical composition od particles during the first (orange) and second (blue) time periods of the campaign showing the black carbon concentration (a) as well as concentrations of sulfate (b), oragnic (c), nitrate (d), cloride (e) and ammonium (f) in non-refractory component of sub-micron particles.

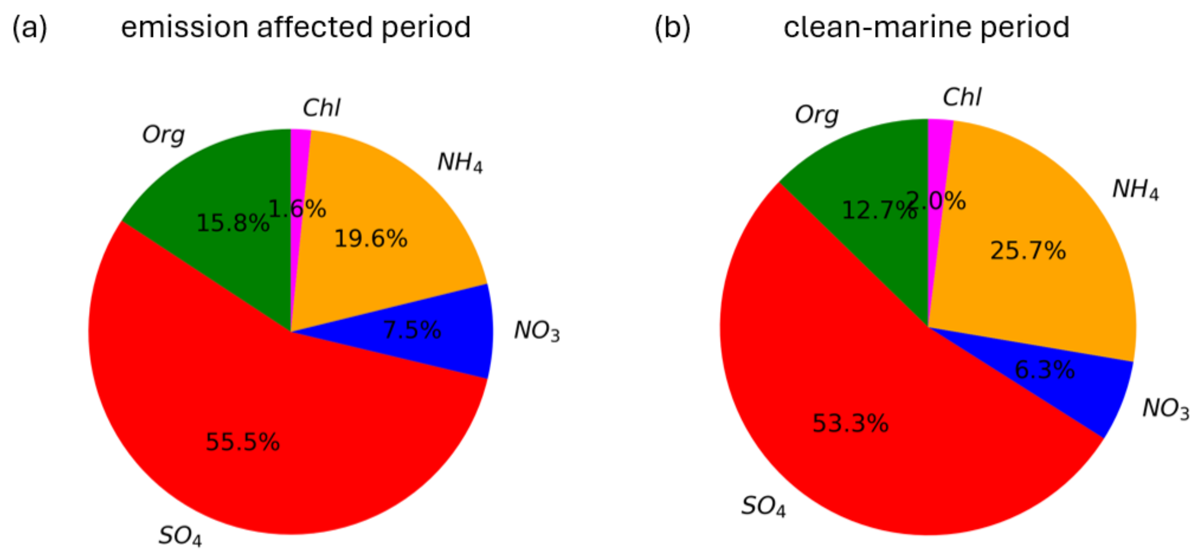

Figure S4: Median chemical composition of non-refractory component of sub-micron particles during the first (a) and second (b) time periods of the campaign.

S4. Nanoparticle ranking

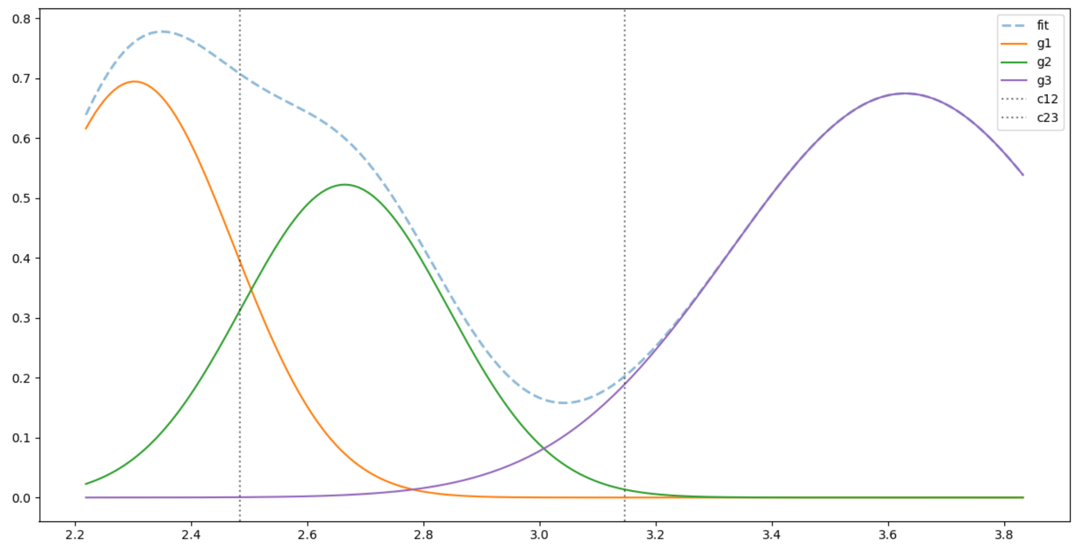

Figure S5: The fitted three modes g1, g2 and g3 on the 2 – 5 nm particle number concentration based on Aliaga et al. 2023.

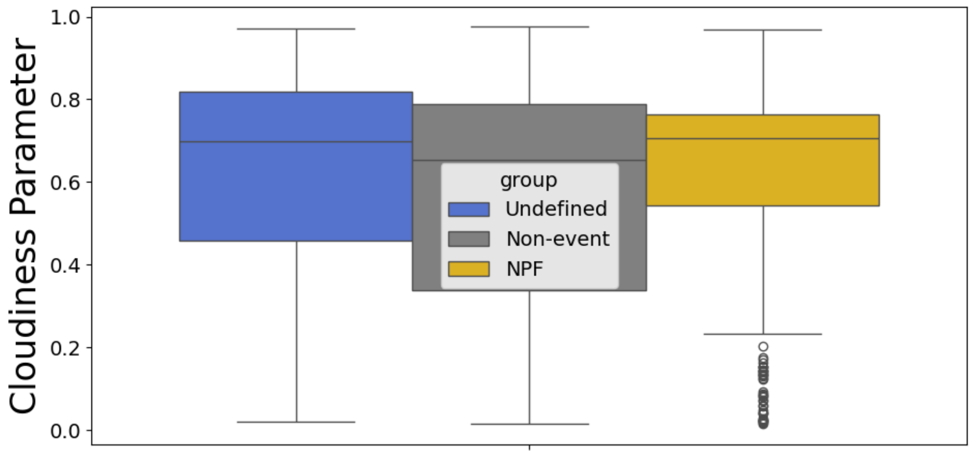

Figure S6: Boxplots of cloudiness parameter measured on the NPF event days (yellow), undefined days (blue), and non-event days (grey).

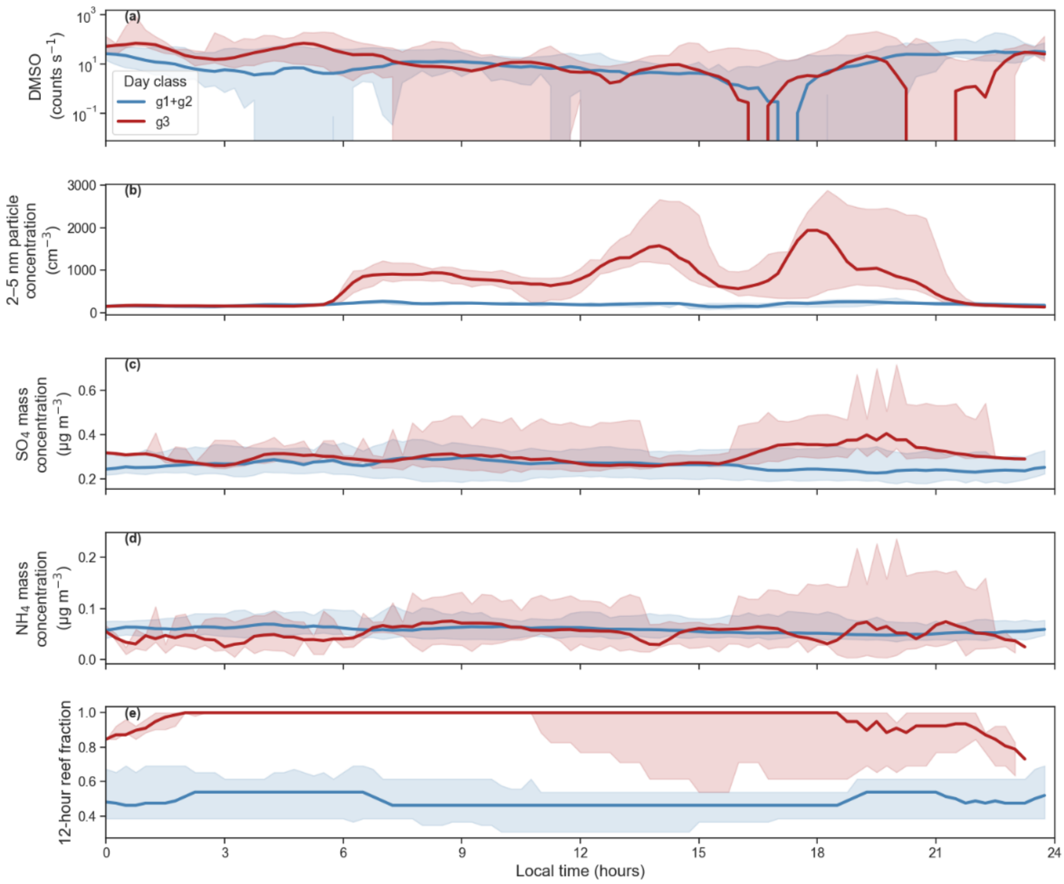

Figure S7: Diurnal variation of the DMSO concentration (a), 2 – 5 nm particle number concentration (b), SO_4 concentration (c), NH_4 concentration (d), and the 12-hour reef fraction (e) during NPF events (red) and combined data for undefined and non-event (blue). Median values are shown by a straight line while shaded areas present the interquartile ranges.

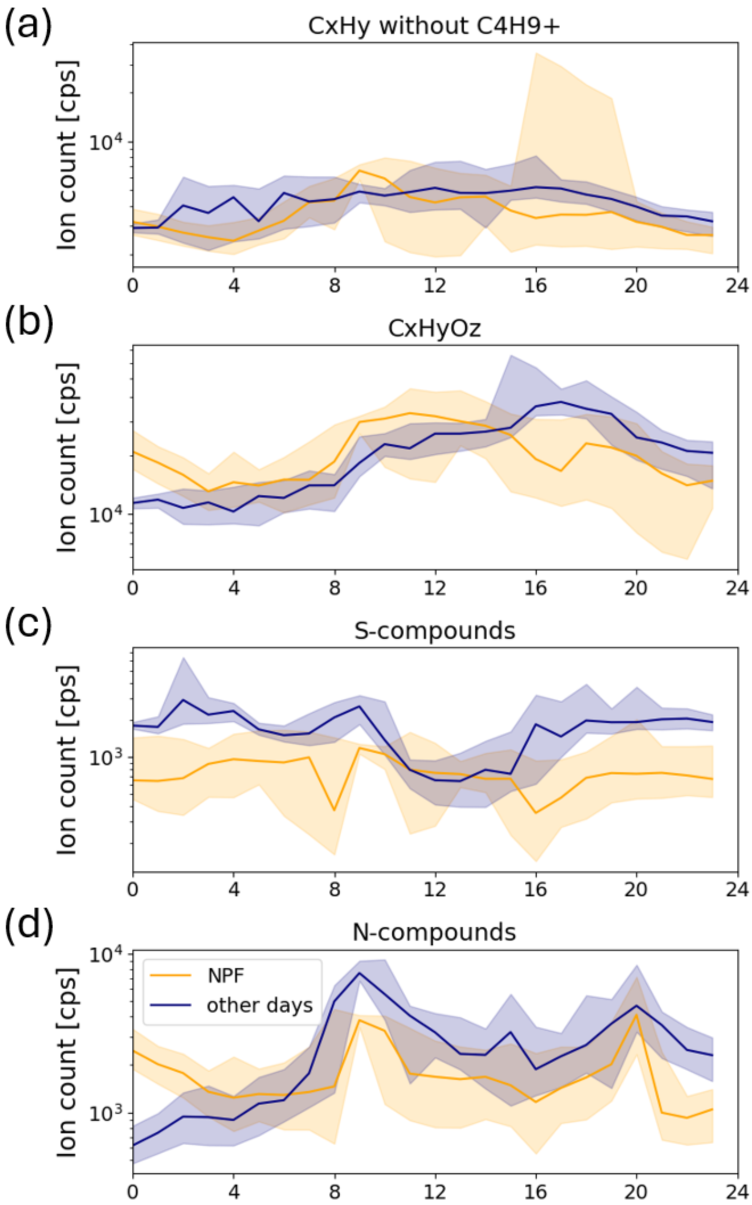

Figure S8: Diurnal variation of the hydrocarbon concentration (excluding $C_4H_9^+$, a), oxidized hydrocarbons (b), S-compounds (c), and N-compounds concentration during NPF event days (yellow) and combined data for undefined and non-event (other days, blue). Median values are shown by a straight line while shaded areas present the interquartile ranges.

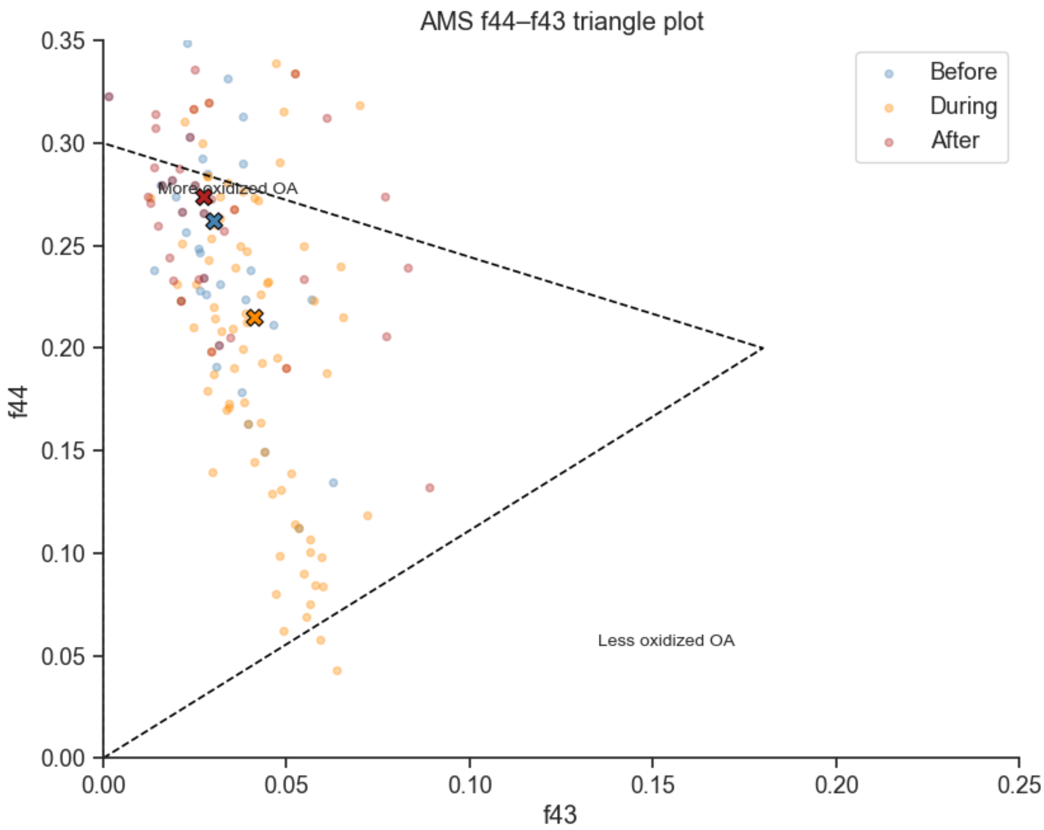

Figure S9: Scatter plot of the f43 and f44 fraction measured by AMS coloured by the measurement time relative to the NPF onset. In case of multiple events detected in a single day, the data before NPF contains only the time before onset of the first NPF event and the data after the NPF contains only the time after the last event of the day.

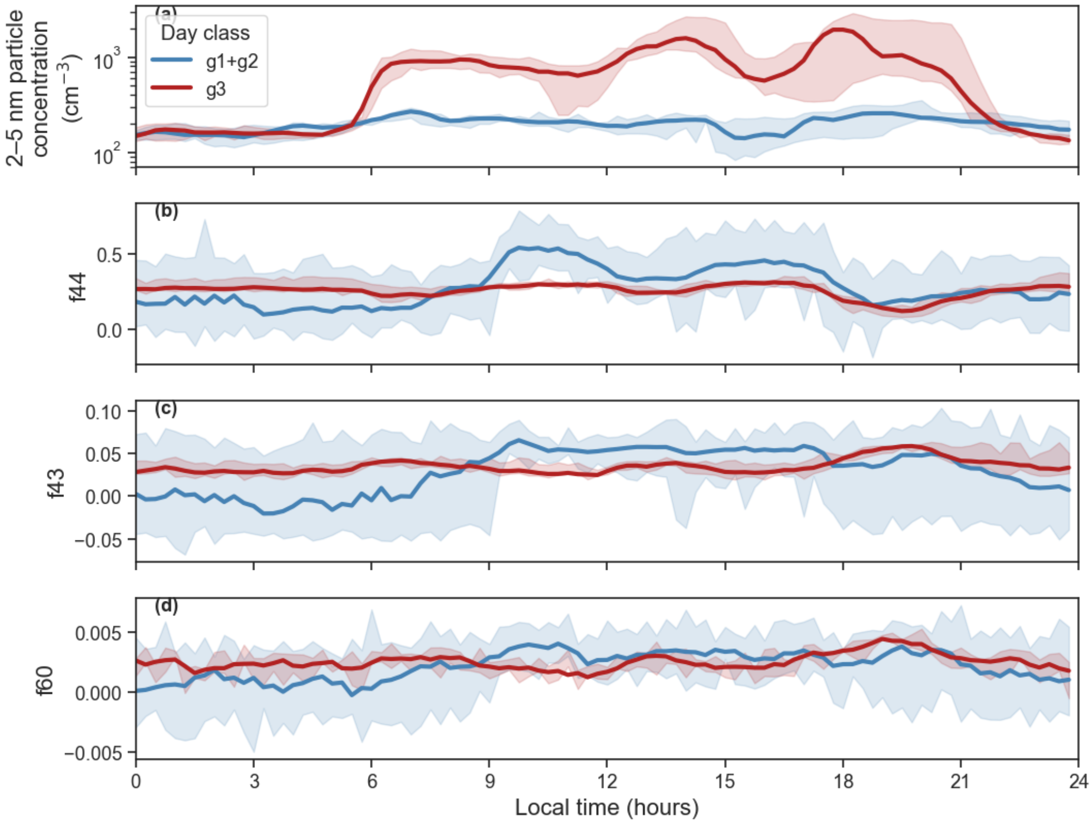

Figure S10: Diurnal variation of the 2 – 5 nm particle number concentration (a), f44 (b), F43 (c), F60 (d) during NPF events (red) and combined data for undefined and non-event (blue). Median values are shown by a straight line while shaded areas present the interquartile ranges.

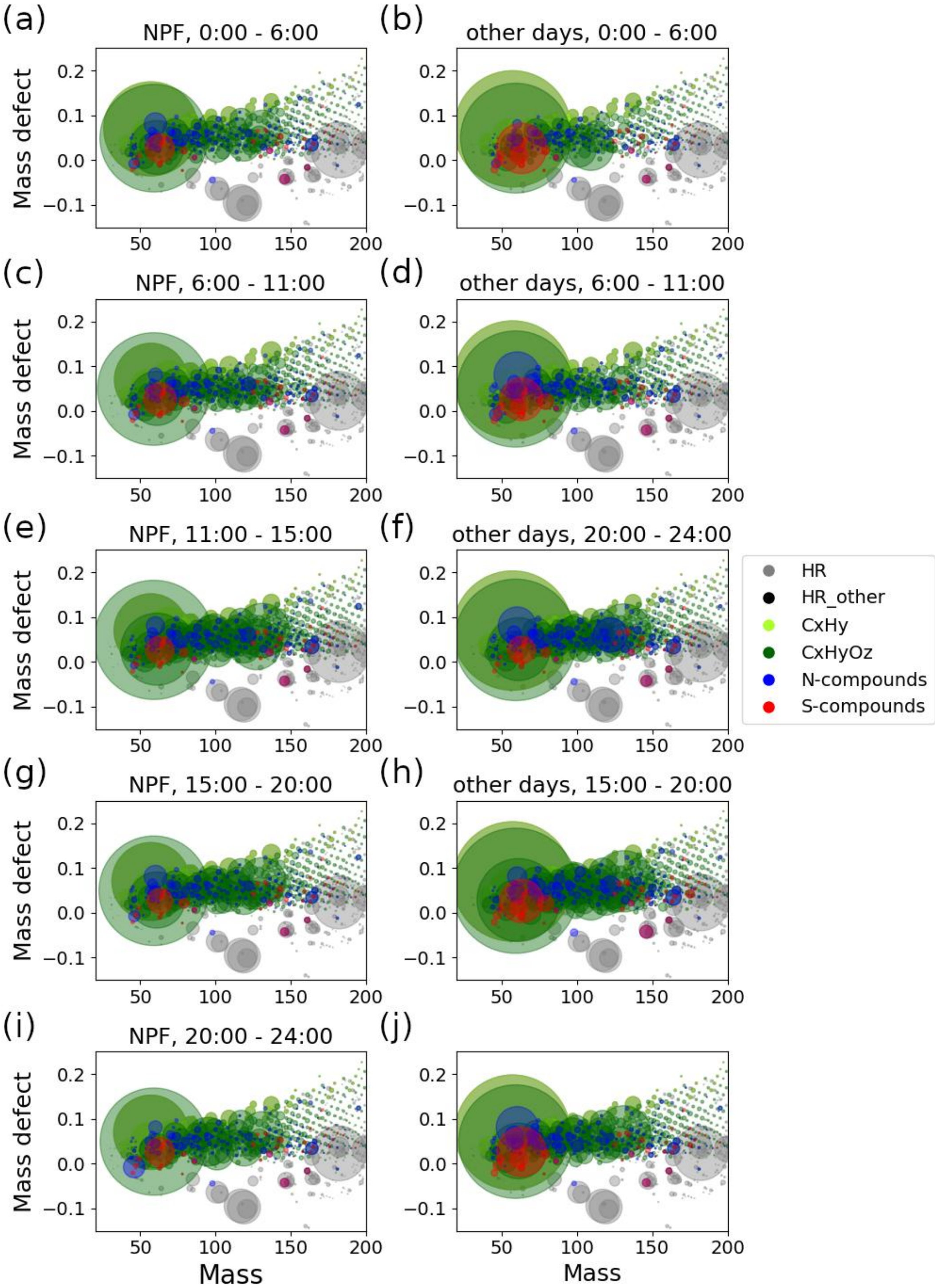

Figure S11: Mass defect plots during NPF event days (a-e) and combined data for undefined and non-event days (other days, f-j) during five different periods of the day: 0:00-6:00 (a, f), 6:00-11:00 (b, g), 11:00-15:00 (c, h), 15:00-20:00 (d, i), and 20:00-24:00 (e, j). The division was based on changes in 2 – 5 nm particle number concentration during NPF event (Fig. S4) representing time before NPF event, during each NPF events, and after the NPF event. 'HR' represent peaks found in the mass spectrum but unidentified while 'HR_other' shows compounds that has been identified but do not fit any other categories (e.g. siloxanes).

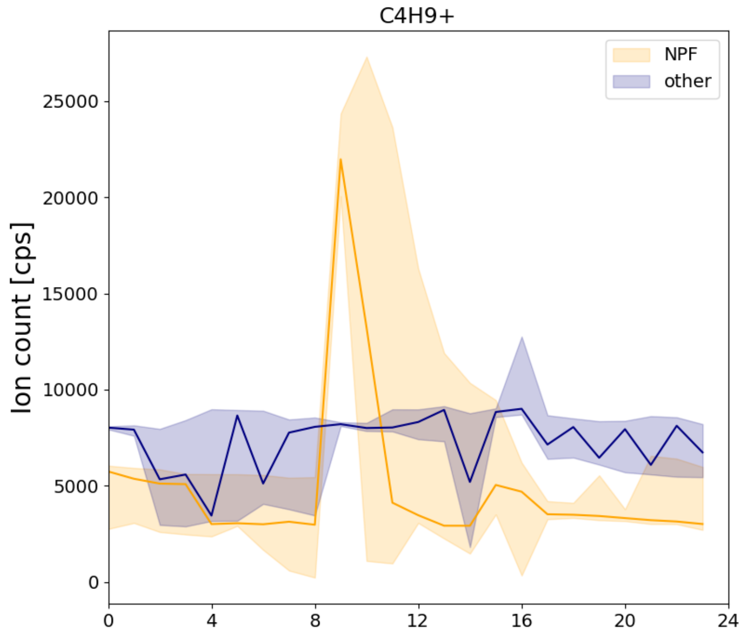

Figure S12: Diurnal variation of the $C_4H_9^+$ concentration during NPF events (yellow) and combined data for undefined and non-event (other days, blue). Median values are shown by a straight line while shaded areas present the interquartile ranges.